Weather and Climate Extremes 16 (2017) 14–22

Contents lists available at ScienceDirect

Weather and Climate Extremes

journal homepage: www.elsevier.com/locate/wace

Evaluating the MSG satellite Multi-Sensor Precipitation Estimate for extreme rainfall monitoring over northern Tunisia

Saoussen Dhib[a,*], Chris M. Mannaerts[b], Zoubeida Bargaoui[a], Vasilios Retsios[b], Ben H.P. Maathuis[b]

[a] ENIT: Université de Tunis El Manar, Ecole Nationale d'Ingénieurs de Tunis, Tunis, Tunisia
[b] ITC: University of Twente, Faculty of Geo-Information Science and Earth Observation, Enschede, The Netherlands

ARTICLE INFO

Keywords:
Rainfall
Extremes
Tunisia
Validation
Meteosat

ABSTRACT

Knowledge and evaluation of extreme precipitation is important for water resources and flood risk management, soil and land degradation, and other environmental issues. Due to the high potential threat to local infrastructure, such as buildings, roads and power supplies, heavy precipitation can have an important social and economic impact on society. At present, satellite derived precipitation estimates are becoming more readily available. This paper aims to investigate the potential use of the Meteosat Second Generation (MSG) Multi-Sensor Precipitation Estimate (MPE) for extreme rainfall assessment in Tunisia. The MSGMPE data combine microwave rain rate estimations with SEVIRI thermal infrared channel data, using an EUMETSAT production chain in near real time mode. The MPE data can therefore be used in a now-casting mode, and are potentially useful for extreme weather early warning and monitoring. Daily precipitation observed across an in situ gauge network in the north of Tunisia were used during the period 2007–2009 for validation of the MPE extreme event data. As a first test of the MSGMPE product's performance, very light to moderate rainfall classes, occurring between January and October 2007, were evaluated. Extreme rainfall events were then selected, using a threshold criterion for large rainfall depth (> 50 mm/day) occurring at least at one ground station. Spatial interpolation methods were applied to generate rainfall maps for the drier summer season (from May to October) and the wet winter season (from November to April). Interpolated gauge rainfall maps were then compared to MSGMPE data available from the EUMETSAT UMARF archive or from the GEONETCast direct dissemination system. The summation of the MPE data at 5 and/or 15 min time intervals over a 24 h period, provided a basis for comparison. The MSGMPE product was not very effective in the detection of very light and light rain events. Better results were obtained for the slightly more moderate and moderate rain event classes in terms of percentage of detected events, correlation coefficient, and ratio bias. The results for extreme events were mixed, with high pixel correlations of R=0.75 achieved for some events, while for other events the correlation between satellite and ground observation was rather weak. MPE data for northern Tunisia seem more reliable during the summer season and for larger event scales. The MSGMPE data have demonstrated to be very informative for early warning purposes, but need to be combined with other near real time data or information to give reliable and quantitative estimates of extreme rainfall.

1. Introduction

North Tunisia has a sub-humid climate in the Northern Mediterranean coastal region and is semi-arid in its southern and eastern parts. The rainfall gauging network of northern Tunisia, 35°2′ N 8°E; 37°2′ N 11°E, is scattered across the area with about 318 stations operational (covering around 113 km^2/station) during the period between 2006 and 2009. For the period of observation (January 2007 to June 2009), the maximum recorded daily rainfall was 136 mm on 12/01/2009. Rainfall actually occurred during five consecutive days from 11/01/2009 to 15/01/2009 and led to extensive flooding in the region. At present, satellite observations covering Tunisia have the potential to furnish near real time rainfall estimations, which are important for predicting weather hazards, flood risks and for environmental management. Rain clouds that produce rain for less than one hour typically cover an area at meso or γ-scale resolution of between 2 and 20 km (Orlanski, 1975). Taking this into account, as well as the poor density of the pluviograph network in some areas,

* Correspondence to: ENIT, LMHE, Campus Universitaire Farhat Hached El Manar, BP 37, Le Belvédère 1002 TUNIS
E-mail address: dhib_saoussen@hotmail.fr (S. Dhib).

http://dx.doi.org/10.1016/j.wace.2017.03.002
Received 26 September 2015; Received in revised form 3 March 2017; Accepted 21 March 2017
Available online 05 April 2017

remote sensing may provide an interesting additional data source for evaluating short duration rainfall spatial variability.

The operational geostationary MSG satellites are very suitable for weather monitoring over Europe and Africa due to their viewing position. According to La Barbera et al. (1993) the high temporal and spatial resolution of the MSG in the visible (VIS) and infrared (IR) wavelength regions allows for the capture of growth and microstructure of precipitating clouds. However, a more direct method to retrieve rain rates is the use of passive microwave (MW) sensors. An example of a MW sensor is the Special Sensor Microwave Imager (SSM/I) measuring microwave brightness temperatures (BT) at different microwave lengths. With this system, a given location on Earth is revisited every six hours (Thomas et al., 1993). Tsintikidis et al. (1997) adopted two statistical methods: the log-linear regression model (Hinde and Demetrio, 1998) and artificial neural networks (NNs) (Nath et al., 2008) to estimate MW rainfall rates. Comparing the results with radar-estimated rain rates, Nath et al. (2008) found that NNs represented the fundamental relationship between BT and rain rates more accurately than the regression model. However, MW sensors underestimate rainfall volumes because of a phenomenon called "beam-filling effect" (BFE), which is very sensitive to cloud type and especially to low cloud (Lafont and Guillemet, 2004). To overcome this problem, the combination of geostationary sensors (i.e., their thermal bands) and microwave sensors, like the SSM/I, has been adopted by several authors (Adler et al., 1993; Vicente, 1994; Levizzani et al., 1996; Todd et al., 1998; Turk et al., 1999). The MPE method was proposed by EUMETSAT in 1999 and is based on combining observations of high temporal and high spatial resolution of the MSG at IR 10.8 μm with higher accuracy rain rate retrieval data received by the SSM/I at 85 GHz (Heinemann et al., 2002). This product was revealed as most suitable for convective precipitation in areas with poor or no radar coverage like Africa and Asia. The underlying assumption is that cold clouds are expected to produce more precipitation than warm clouds (Heinemann and Kerényi, 2004).

Sánchez-Moreno et al. (2008) performed a rainfall estimate comparison for the semi-arid country Cape Verde. A single storm was studied and data from different satellite sensors were compared, drawing on the combined Microwave imager (TMI) algorithm 2A12, precipitation radar (PR) 2A25, the TRMM 3B42 product, and the MPE method, while using ground data as the reference. It was found that TRMM 3B42 underestimates the amount of rainfall, while PR analysis 2A25 and MPE were most similar to the ground data. MSGMPE proved reasonable accurate at estimating daily or decadal rainfall amounts over the islands (totaling 4033. km^2 in land surface). The MSGMPE images are freely available at the EUMETSAT website and can be directly ingested and analyzed by the ILWIS Open GEONETCast Toolbox (Maathuis et al., 2011). Another inter-comparison of MSGMPE with RFE2.0, TAMSAT, and in situ station data was undertaken by Ataklti (2012), who showed that MSGMPE 3 km data gave a good estimation of areal rainfall in the Tigray region of Northern Ethiopia during the rainfall season in 2010.

The main objective of this study is to investigate the use of MSGMPE satellite data to estimate very light to moderate rain classes and, especially, substantial and extreme daily rainfall events in Northern Tunisia. This was done by comparing satellite estimates of a collection of rainfall events that occurred during the period 2007–2009 over Northern Tunisia, to rainfall estimates derived from the surface rain-gauge network. The paper is organized in three parts: part one includes materials and methods, including a description of the study area (North Tunisia). Part two presents the results and discussion. The final part reports on conclusions and perspectives of the research.

2. Materials and methods

2.1. Ground data

The study area covers the north of Tunisia. It is divided into three geographical sub regions: the Medjerda River watershed (W-5), the Meliane River watershed (W-4) and the smaller watersheds of the northern coastal basins (W-3). The region covers an area of almost 36,000 km^2. To the north and east it is bounded by the Mediterranean Sea, to the west by Algeria and to the south by the Atlas Mountain range in the center of Tunisia. The study period extended from January 2007 to August 2009. Daily rainfall data were provided by the DGRE (General Direction of Water Resources). Three sub periods are considered: January 2007 to September 2007, September 2007 to September 2008, and September 2008 to September 2009.

Fig. 1 depicts the rainfall stations' locations in the study area. Their elevation range indicates important variations, with high orographic areas located in the southwestern part. The number of operational stations is listed by sub region and observation period in Table 1.

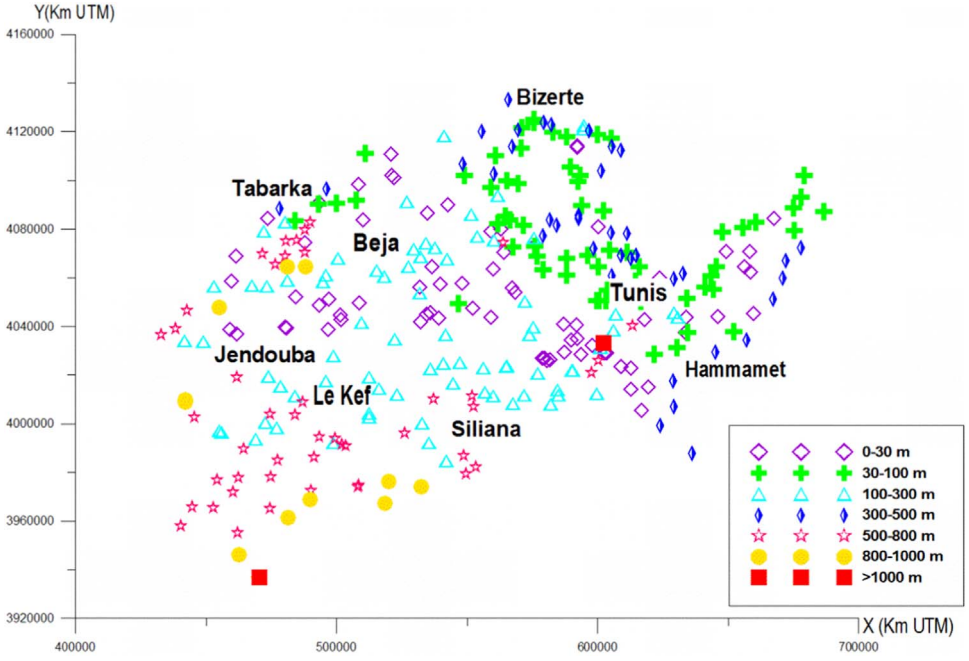

Fig. 1. The study area (North Tunisia) and rainfall station network. The symbols represent the elevation of rainfall stations, which varies between 1 and 1020 m.

Table 1
Station network size by year and region.

	2006/2007	2007/2008	2008/2009
Watershed 3	67	67	43
Watershed 4	116	117	111
Watershed 5	148	144	142

Before evaluating extreme events, the first 10 months (from January to October 2007) were used to evaluate the performance of MSGMPE for very light and moderate rainfall events. This classification is based on a threshold S having been registered in at least one station: very light event ($0 > S > 10$ mm/day), light ($10 > S > 20$ mm/day), slightly moderate ($20 > S > 30$ mm/day), or moderate ($30 > S > 50$ mm/day). In total, 185 events were identified. They were classified into two seasons according to their time of occurrence: dry summer season (May to October) and wet winter season (November to April). Out of 185 events, 100 occurred during the wet season and 85 during the dry season (Fig. 3).

To identify heavy rainfall events, the proposed selection criterion was a precipitation threshold S occurring at least at M stations. Dealing with heavy rainfall, a threshold of S=50 mm/day was selected. To choose M, we refer to Orlanski (1975), who indicated that the scale of variability for thunderstorms corresponds to 1 km for cumulus convective rainfalls. As the minimum distance between stations in the study area is 5 km, the value M=1 was retained. Thus, 77 extreme rainfall events (days) were identified. The selection of heavy rainfall events brought two aberrant values in the gauge data to light, with rainfall exceeding 100 mm in a single station while the rainfall recorded in neighboring stations did not exceed 10 mm. These anomalies were reported to DGRE that verified and corrected these values in their rainfall annual.

Of the 77 events, 35 occurred during the summer season and 42 during the winter season. The most extreme rainfalls occurred at the end of the dry season, on 24/09/2007, 13/10/2007, and 13/09/2008 with 62, 33, and 18 ground stations, respectively, receiving more than 50 mm that day. In fact, in all three cases, these extremes were included in rainfall periods of 72 h (three days). The number of stations meeting the selection criteria (S=50 and M=1) is presented in Table 2 for both the dry and wet seasons. For the wet season the most important events were from 08/03/2007 to 11/03/2007, from 12/01/2009 to 13/01/2009, and from 09/04/2009 to 13/04/2009 (Table 2).

2.2. Interpolation

The spatial interpolation of the light and moderate ground rainfall data was undertaken employing a Moving average (inverse distance weighted) method using ILWIS. The extreme events were interpolated using two interpolation methods: Moving average method and ordinary kriging. The reason for this was purely operational: due to the large number of events to be interpolated, the manual (per event) interpolation process in ILWIS was replaced with an automatic estimation based on especially created FORTRAN code (Bargaoui and Chebbi, 2009), using the kriging interpolation method. Kriging was applied to analyze summer period events and inverse distance weighting to the winter period events.

The kriging interpolation method is derived from the regionalized variables theory (Oliver and Webster, 1990). It requires a semi-variogram model analysis to identify the type of semi- variogram model, as well as its sill and range (Stein, 1999), which represent the scales of variability. An automatic method was adopted for estimating model parameters (sill and range). The method is presented in Bargaoui et al. (2013). Moving average (Mav) applies a weighted averaging on point values of the input point map. There are two weight functions available in ILWIS. The inverse distance method may be selected when the measured point values are very accurately known or, otherwise, the linear decrease method, which decreases the impact of uncertain or erroneous measurements, can be used (Ilwis help 1999). The limiting distance (range) is automatically detected by ILWIS.

A comparison between the two interpolation estimates obtained for the dry season event of 18/05/2008 resulted in a discrepancy in the range estimation of about 20%: 23.6 km by Ilwis, compared to 20 km by kriging. The inverse distance algorithm provided a better correlation with kriging estimates (R=0.95) than the linear decrease method (R=0.89) did. Furthermore, the inverse distance method performed better regarding the root mean square error coefficient (RMSE), which was 2.5 mm/day (compared to 3.8 mm/day using the linear decrease interpolation method). As a result, the moving average method using an inverse distance weighting was further adopted for interpolating the rainfall maps corresponding to the winter season.

Fig. 2 reports three well distinguishable experimental semi variograms (24/09/2007, 13/10/2007, and 13/09/2008) out of a total of 77. They were adjusted to form spherical models (Berolo and Laborde, 2003) which are depicted in Fig. 2. The three variogram fitting results were within ranges of respectively 22, 17, and 18 km with sills of 480, 180, and 280 $(mm/day)^2$.

On the other hand, the presence of a "hole effect", characterized by important fluctuations around the sill, is outlined for some variograms. According to Bosser (2011) this is a characteristic of heterogeneous data, and in our study occurred during the 24/09/2007, 13/10/2007, and 14/10/2007 events. However, we did not analyze this aspect and assumed a spherical model for all events. The quality of variogram fitting was assessed using cross validation. Ranges varied between 15 km and 25 km. A typical range of 20 km was adopted in this study to perform the kriging interpolations.

2.3. Satellite databases

The satellite rainfall database was constructed from data orders obtained through the internet from the UMARF archive of EUMETSAT. Since the daily gauge data on the ground are always monitored from 7 am one day to 7 am the next, local time in Tunisia, it was necessary to perform a temporal re-scaling of the 15 (or in some cases 5) minute duration satellite images. This step was automated using the ILWIS scripting language. A *mapcross* or overlay operation was further performed using the ILWIS *resample* routines to develop an equally gridded geolocation for both the ground observations and satellite rainfall maps.

2.4. Map intercomparison

Firstly, using pixel estimations with a three km resolution, Pearson correlation coefficients were estimated to compare the ground rainfall maps with the satellite rainfall estimations on an event by event basis. The generated scatter plots of the events' average spatial rainfall were examined to assess the general goodness of fit. Next, a comparison of map quantiles was performed through the examination of quantiles of the scatter plot for a given event. Additionally, map aggregations to resolutions of 30 km and 50 km were performed in order to examine the sensitivity of the performance criteria to spatial resolution. Finally, to understand the influence of the interpolation methods for matching ground and satellite estimations, we inverted the interpolation methods used for the dry and wet seasons of the extremes events. The correlation coefficient, ratio bias and RMSE coefficients were used as criteria of performance.

3. Results

3.1. Very light and moderate rainfall events

Fig. 3 reports on the statistic results of the evaluation of satellite estimations versus ground estimations for the 185 events and the

Table 2
Occurrences of heavy rainfall during wet and dry seasons in study period.

Wet season				**Dry season**			
Date	Number of stations > 50 mm	Average ground (mm/d)	Average satellite (mm/d)	**Date**	Average ground (mm/d)	Average satellite (mm/d)	Number of stations > 50 mm
01/02/2007	1	9.2	0	**13/09/2007**	2.8	5	2
26/02/2007	1	7.4	0	**14/09/2007**	1.7	0.6	1
08/03/2007	62	28	18	**17/09/2007**	3.4	6	1
09/03/2007	41	21.2	24	**23/09/2007**	3.1	0	3
10/03/2007	5	9.3	0.5	**24/09/2007**	22.1	49	62
11/03/2007	17	19.6	0	**25/09/2007**	5.6	0	16
12/03/2007	3	9.3	0.1	**26/09/2007**	1.8	0	1
22/03/2007	2	10.3	7	**27/09/2007**	0.5	0	1
16/04/2007	1	6.3	0	**07/10/2007**	3.3	0	3
18/04/2007	1	0.6	0	**12/10/2007**	1.5	0	1
11/12/2007	1	8.9	0.3	**13/10/2007**	1.5	0	33
12/12/2007	1	7.1	0	**14/10/2007**	4.4	0	14
14/12/2007	1	3.7	0.2	**15/10/2007**	2.2	0	1
27/03/2008	11	8.4	0.1	**16/10/2007**	8.3	9	2
31/03/2008	1	17.5	9.4	**18/10/2007**	1.1	0.3	1
01/04/2008	2	7.4	0	**19/10/2007**	0	0	0
17/112008	2	6	0	**21/10/2007**	0	0	7
16/11/2008	3	8.5	2.4	**22/10/2007**	0	0	3
18/11/2008	0	3.8	4.1	**30/10/2007**	3.9	1	1
17/12/2008	8	8.3	3	**11/05/2008**	8.2	1	0
18/12/2008	2	6.2	0	**12/05/2008**	11.4	16	1
09/01/2009	2	2.4	0.2	**18/05/2008**	11	17	1
12/01/2009	140	56.2	4.3	**06/09/2008**	10.2	0	2
13/01/2009	60	24.5	0	**12/09/2008**	2.5	0	2
20/01/2009	1	7.9	45.3	**13/09/2008**	18.1	0	18
21/01/2009	1	7.7	0	**14/09/2008**	7.3	0	7
11/02/2009	4	8.9	0	**15/09/2008**	1.4	0	1
23/02/2009	11	9.8	0	**25/09/2008**	3	0	1
24/02/2009	0	7.5	51.6	**30/09/2008**	10.3	2	4
06/03/2009	17	15	0	**03/10/2008**	12.1	0	1
07/03/2009	2	6.3	0	**17/10/2008**	4.1	0	1
08/04/2009	1	11.8	5.6	**22/10/2008**	6	1	7
09/04/2009	45	22.8	0	**15/05/2009**	10.5	12	11
10/04/2009	16	8.2	0	**31/05/2009**	6.8	0	1
11/04/2009	32	25.3	6				
12/04/2009	51	14.5	0				
13/04/2009	6	6.4	0				
18/04/2009	1	4	0.5				
19/04/2009	1	13.1	24.7				
21/04/2009	5	8.1	0				
22/04/2009	14	15.1	3.5				
23/04/2009	1	5.2	10.6				

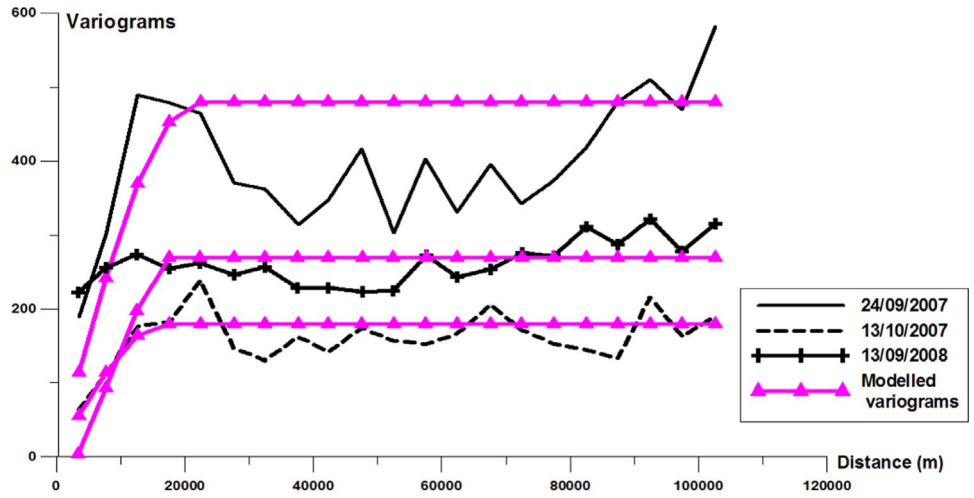

Fig. 2. Sample and modeled variograms for basin 5 (3 events during wet season). The lines incorporating triangles represent the adjusted variograms. The three other lines represent the experimental semi variograms for 24/09/2007 (continuous line), 13/10/2007 (dotted line), and 13/09/2008 (the 'plus' patterned line).

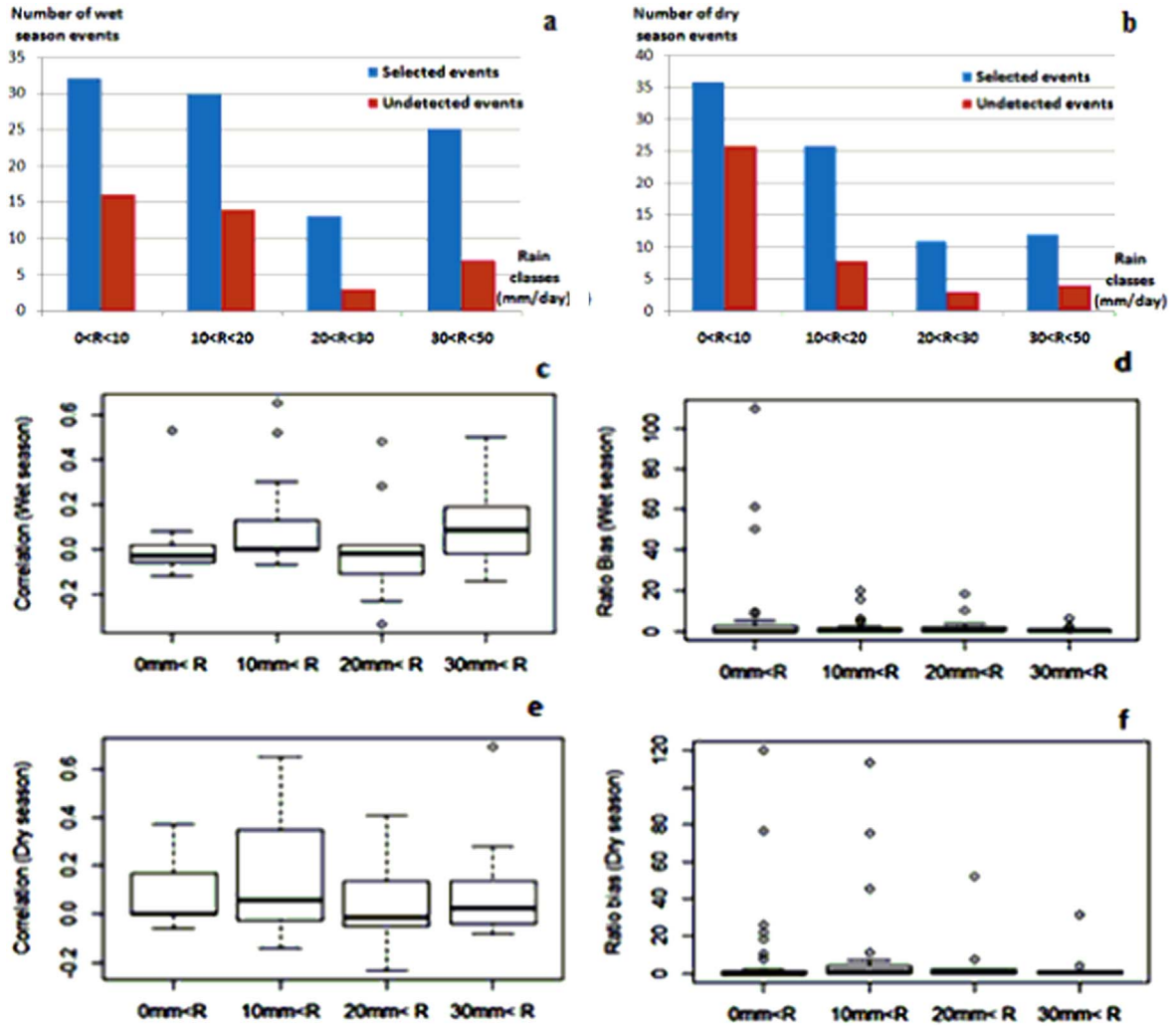

Fig. 3. The statistic coefficient for each class of rainfall event: the number of selected and undetected events during the wet season for each class (a), the number of selected and undetected events during the dry season for each class (b), correlation coefficients of all the classes during the dry season (c), ratio bias of all the classes during the dry season (d), correlation coefficient of all the classes during the wet season (e), ratio bias coefficient of all the classes during the wet season (f).

different rainfall classes at a three km spatial resolution. MSGMPE shows a weak capacity to detect very light events (at least one station recorded rainfall of more than 0 and less than 10 mm/day). This weakness is seen in both seasons, with 50% and 72% of events remaining undetected during the wet season (Fig. 3a) and dry season (Fig. 3b), respectively. The correlation coefficient of this class is very weak with an average of 0 for both seasons. The ratio bias coefficient (average by satellite/average on the ground) is overestimated in both

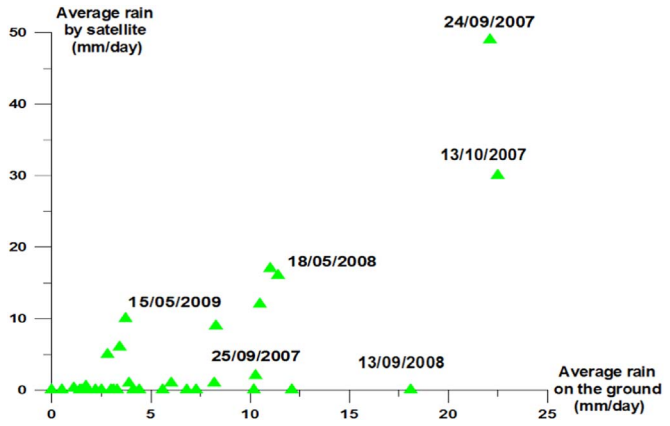

Fig. 4. Comparison of spatially averaged precipitation between ground stations and satellite estimations for the summer period (36 events).

seasons (Figs. 3d and f). For the light rain class (10 mm/day < R < 20 mm/day) MSGMPE detected rainy events better during dry season, with only 31% of events remaining undetected. During the wet season 47% of events remained undetected. The correlation coefficients for the light rain events are superior to those for the very light rain events (Figs. 3c and e).

The highest percentage regarding detection is found in the slightly moderate and moderate classes, with a variation of 67–77% for both seasons. The ratio bias coefficients of these two classes are more or less similar with better correlation coefficients occurring in the moderate class.

3.2. Extreme events

3.2.1. Comparison of summer season rainfall events

Fig. 4 depicts the scatter plot of satellite estimations versus ground estimations for the 35 events selected during the summer season at a 3 km spatial resolution. It indicates a slight average under-estimation of the rainfall by the satellite algorithm of 8%.

Although some events show a high correlation between ground and satellite observation, there are 16 events for which the satellite estimation indicates zero rain (in particular 13/09/2008, 03/10/2008, and 25/09/2007). For certain events a high discrepancy is reported, as for example for the 24/09/2007 event. For the event that occurred on 18/05/2008 and was quite well estimated (Fig. 4), a map comparison was undertaken. The spatial gradients in these two maps are similar (Figs. 5a and b) with a correlation coefficient of 0.51. A

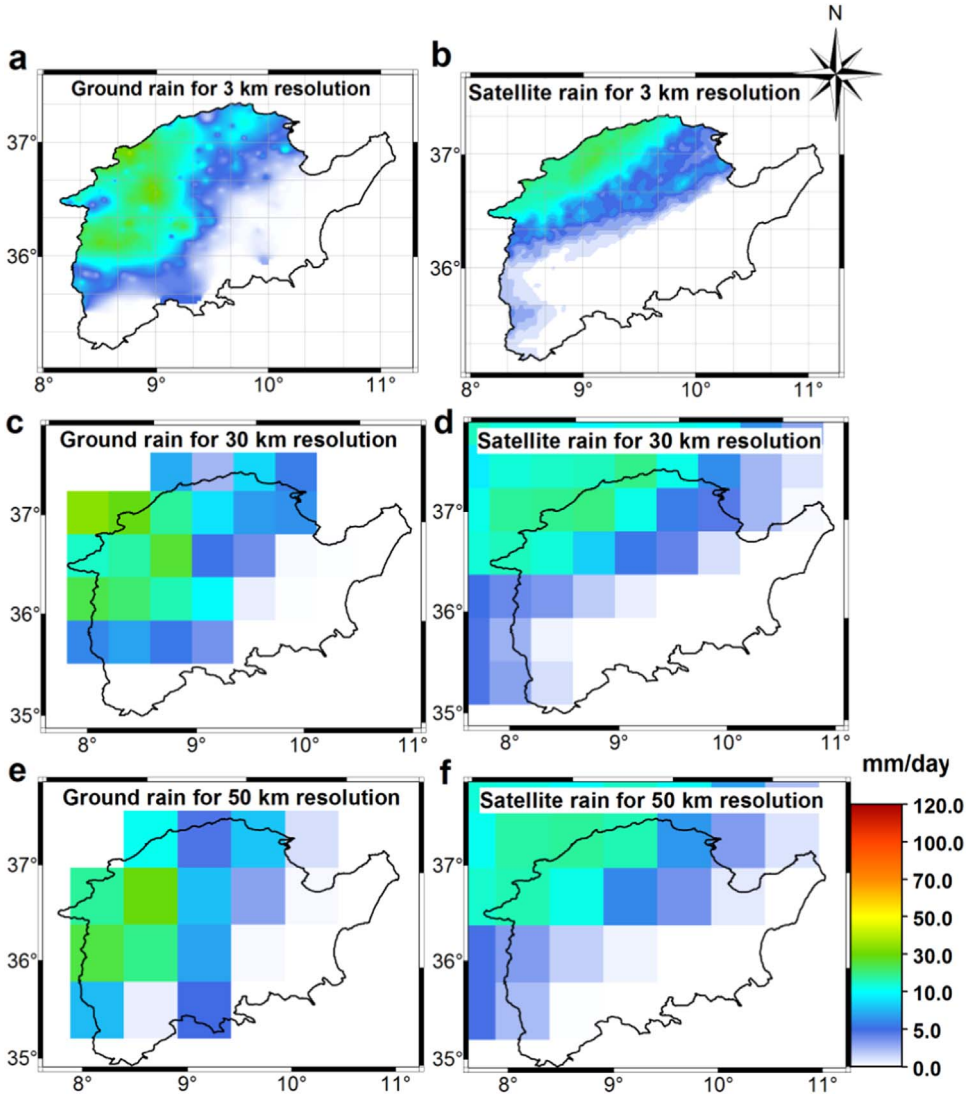

Fig. 5. Comparison of gauge and satellite rainfall occurring on 18/05/2008 at different spatial resolutions (3 km, 30 km and 50 km): in situ rain at 3 km resolution (a), satellite estimated rain at 3 km resolution (b), in situ rain at 30 km resolution (c), satellite rain at 30 km resolution (d), in situ rain at 50 km resolution (e), satellite rain at 50 km resolution (f). Maximal rainfall recorded on the interpolated ground map (Max.Gr.) and by satellite (Max.Sat.) at 3 km spatial resolution is about 68 mm/day and 25 mm/day, respectively.

subsequent spatial aggregation to a resolution of 30 km raises the Pearson correlation coefficient to 0.61 (Figs. 5c and d).

In Fig. 6a, pixel frequency curves are compared for the 18/05/2008 event. This reveals a serious underestimation of rainfall by the satellite. Additionally, the percentage of pixels with zero rainfall is abnormally high in the satellite estimation. On the other hand, as expected using the MPE method, the scatter plot of quantiles restitutes a good determination coefficient at 3 km resolution (R^2=0.92, in Fig. 6b).

Fig. 6a reports the frequency curves at 30 km resolution. The underestimation by satellite products is still visible. On the contrary, the scatter plot of the quantiles (Fig. 6a) reflects good agreement (R^2=0.96). Aggregating the maps to a scale of 50 km (Figs. 5e and f) results in very similar maps (Fig. 6b), with an increase in the correlation coefficient from 0.61 to 0.72.

Events that remained undetected by satellite can be divided into two types, based on an analysis of the gauge rainfall data: 1) very heavy and extreme rainfall events exceeding 100 mm/day but occurring on very localized and small areas, corresponding typically to a local thunderstorm pattern (Fig. 7a), and 2) generalized low rainfall events, where the maximum station or point rainfall recorded not exceeding 15 mm/day over large surfaces (Fig. 7b).

Based on the number of stations with recorded rainfall exceeding 50 mm/day, we note that most of the events, undetected by the satellite, correspond to days where heavy rainfall either occurred in just one or two stations (13 events), or occurred in localized spots (four events), or in high orography mountain areas (one event). In the dry summer season, only one important rainfall event (on 13/09/2008, when 18 stations recorded rainfall exceeding 50 mm/day with an average of 50.9 mm) was completely undetected using the MSGMPE satellite data. The reasons for this non-detection can be multiple (atmospheric, physical, but also satellite recording and data processing and production chain issues) and would need more analysis and evaluation in future research.

3.2.2. Comparison of winter season rainfall events

In Fig. 8, the interpolated in situ daily averages are compared with the satellite daily average estimates. During the wetter winter months, we also observed a significant underestimation of rainfall based on MSGMPE. In addition, only 24 out of 42 events were detected by satellite. For 14 events, out of 24, the spatial average rain estimated by satellite exceeded 3 mm/day. For the remaining events, it was less than 1 mm/day.

In order to complete the data inter-comparison, Fig. 8 reports the standard deviations versus the averages at spatial resolutions of 3 and 30 km, both of ground and satellite estimations. The two scatter plots of Fig. 8 are in good agreement for all events except for four cases: 12/01/2009, 20/01/2009, 24/02/2009, and 19/04/2009. To help understand the extent of the discrepancy between ground and satellite estimations, Fig. 9 shows some of the corresponding rainfall maps. It is clear that satellite rainfall amounts (Fig. 9b) are completely out of the observed rainfall (Fig. 9a) range for 12/01/2009, despite the similarity in the spatial variability structure. For 24/02/2009 (Fig. 9f) neither the rainfall range nor the variability features conform to the ground estimations (Fig. 9e).

For 20/01/2009 (Fig. 9c), the spatial extent of the rainfall is overestimated by satellite estimations (Fig. 9d).

Correlation coefficients between average estimates improved at 30 km and 50 km resolutions. For example, the correlation coefficient of 19/04/2009 increased from 0.38 at 3 km resolution to 0.43 at 30 km resolution, and to 0.51 at 50 km resolution, thus showing a slight

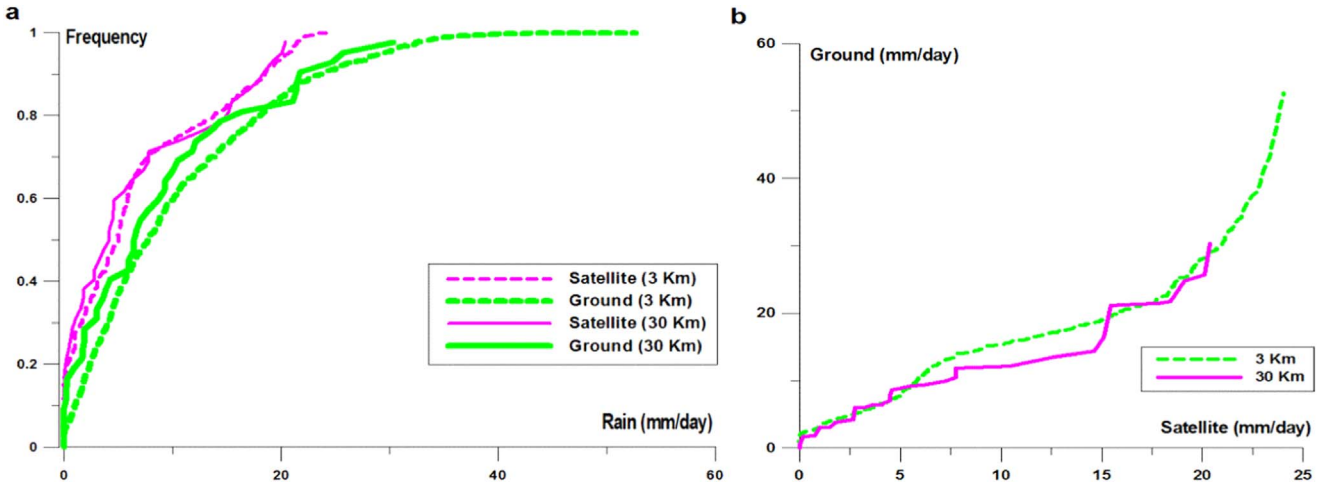

Fig. 6. (a) Cumulative frequency curves for rainfall event 18/05/2008 on the ground (thick curves) and by satellite (thin curves) for 3 km (interrupted curves) and 30 km (continue curves) spatial resolutions; (b) Statistical quantiles for rainfall event 18/05/2008 at different spatial resolutions (3 km and 30 km).

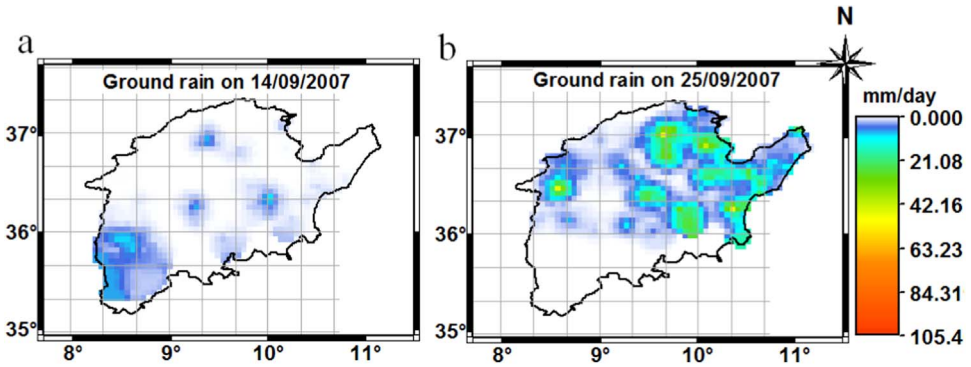

Fig. 7. Examples of undetected rainfall events. (a) Max.Gr.=14 mm/day, Max.Sat.=1 mm/day, (b) Max.Gr.=43 mm/day, Max.Sat.=0 mm/day.

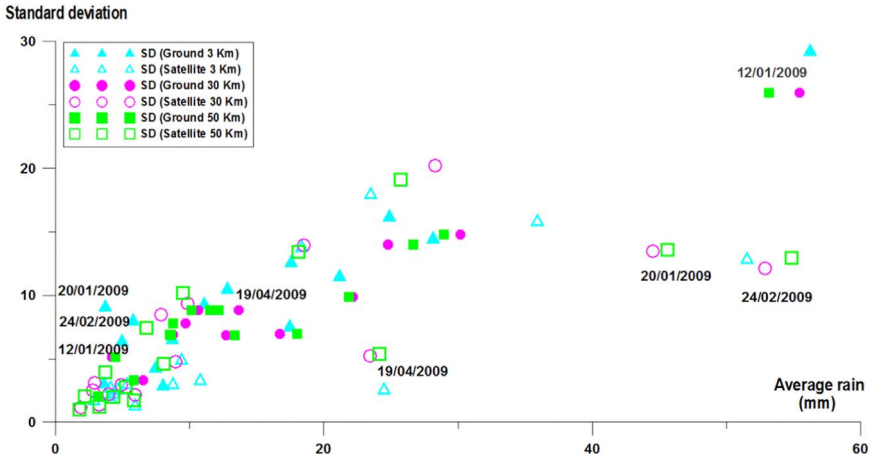

Fig. 8. Comparison of spatially averaged precipitation between ground station measurements and satellite estimations for the wet winter period (42 events). The filled symbols (triangle, circle, and square) represent the average ground rainfall and the vacuum symbols represent the average satellite rainfall at resolutions of, respectively, 3 km, 30 km, and 50 km.

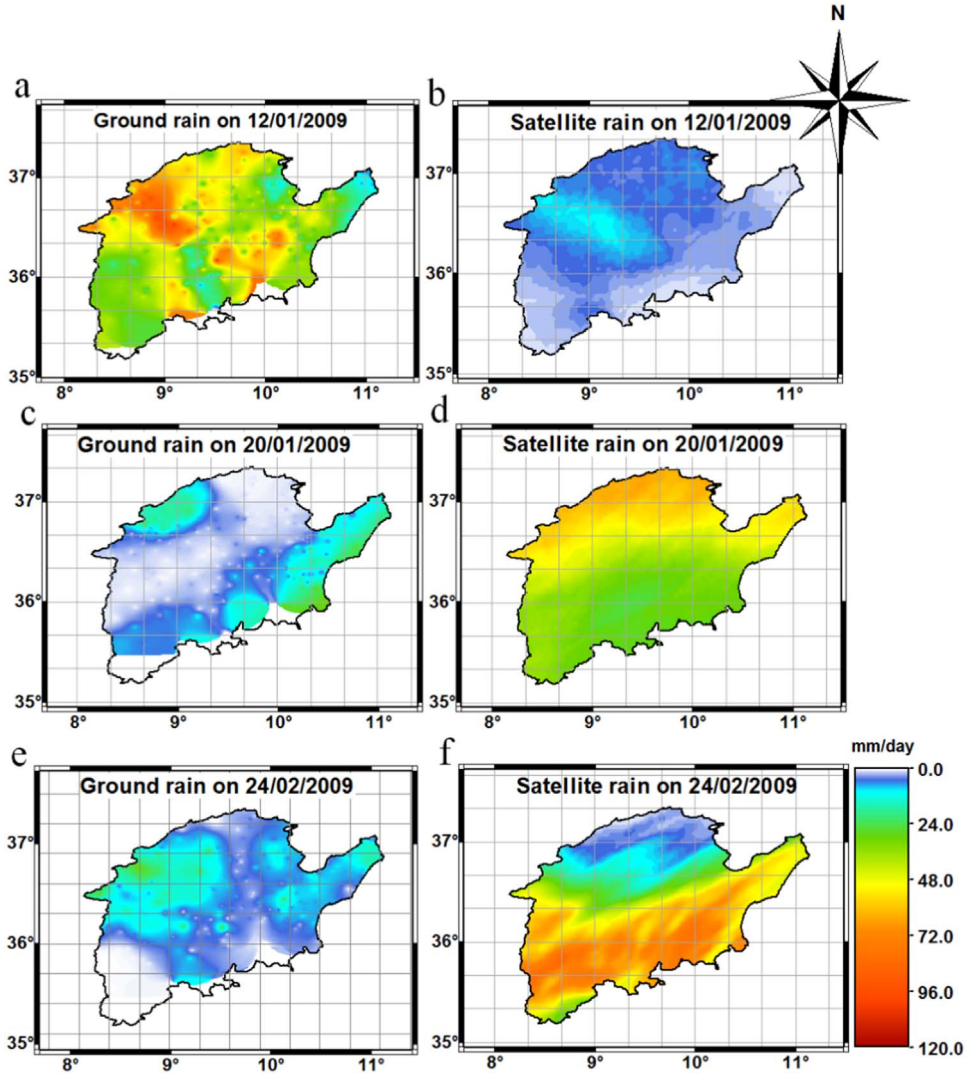

Fig. 9. Comparison of satellite and ground-based rainfall for 3 events during the winter season. (a) and (b) represent the 12/01/2009 event regarding satellite and ground rainfall, respectively. (Max.Gr.=124 mm/d, Max.Sat.=11 mm/d), (c) and (d) represent the 20/01/2009 event regarding satellite and ground rainfall, respectively. (Max.Gr.=30 mm/d, Max.Sat.=70 mm/d), (e) and (f) represent the 24/02/2009 event regarding satellite and ground rainfall, respectively. (Max.Gr.=25 mm/d, Max.Sat.=70 mm/d).

correction at the 50 km resolution. However, the correlation coefficients of the 12/01/2009, 20/01/2009, and 24/02/2009 events remained low (Fig. 8).

The events that remained undetected by the satellite in the wet season differed and represented either rainfall widely scattered in space (2 events), or rainfall very localized in areas of high elevation (8 events),

or events restricted to one or two ground stations receiving more than 50 mm/day rainfall (9 events). In particular, 5 non-detected events are characterized by more than 15 stations receiving more than 50 mm/day rainfall, revealing a certain inadequacy in MSGMPE satellite estimates for these atmospheric situations and rainfall systems. Further analysis of these events, using other MSG data such as daytime microphysical color scheme composite and physical cloud property data, are required to shed more light on the non-detection issue.

3.2.3. Comparison between the interpolation methods (inverse distance and kriging)

The results indicate a better performance of the Inverse distance method for the correlation coefficient in the dry season and for both seasons in terms of ratio bias and RMSE. However, the kriging method presented slightly better correlation coefficients for events in the wet season.

4. Discussion and conclusions

The main goal of this study was to compare the near real time satellite rainfall estimates from MSGMPE with ground station rainfall gauge observations to assess the accuracy of the MSGMPE for the estimation of extreme rainfall in Northern Tunisia. Because MSGMPE is a near real time product, it can be quite useful as an early warning system in case of heavy rainfall occurrences and subsequent water hazards, such as flooding and inundation. Another goal of this study was to compare the reliability of MSGMPE multisensory precipitation estimates for two different seasons (the dry summer and wet winter). Ten months from January to October 2007 were used to evaluate the performance of MSGMPE for very light to moderate rainfall classes. In all, 185 events were identified and interpolated using the inverse distance method. The MSGMPE product displayed weak skill in the detection of very light and light events. Better percentage of detection was obtained for slightly moderate and moderate classes, with better correlation and ratio bias coefficients. Large and extreme rainfall events were identified using a threshold of 50 mm/day, at least observed at one ground station. The in situ database of daily rainfall data for the period from January 2007 to August 2009 was interpolated using the ordinary kriging method for the dry period May to October and the moving average method for the wet period November to April. It became clear that aggregation of the MSGMPE estimates, from an original sample resolution of 3 km to resolutions of 30 km and 50 km, introduced a moderate improvement. We also observed that events of extreme rainfall, but with a low geographic extent (recorded rainfall of > 50 mm/day, but detected by less than 3 stations) were underestimated by the MPE satellite product. This was also the case for events characterized with high rainfall heterogeneity within the pixels. In general, we can confirm an underestimation of rainfall by the MSGMPE algorithm (77 events), except for five events, which were overestimated. Based on the percentage of events detected by the satellite, we conclude that the MPE method is more suitable in North Tunisia during the drier summer period, when convective rainfall prevails. Finally, we suggest this method to be combined with other data and/or information, in order to produce more reliable extreme rainfall estimations for all weather situations in Tunisia.

Funding

This work was supported by the University of Tunis-El Manar (internship support in ITC).

Acknowledgements

Authors wish to thank the General Direction of Water Resources of Tunisia for providing the ground rainfall data, and staff at ITC and ENIT for their assistance.

Appendix A. Supporting information

Supplementary data associated with this article can be found in the online version at doi:10.1016/j.wace.2017.03.002.

References

Adler, R.F., Negri, A.J., Keehn, P.R., Hakkarinen, I.A., 1993. Estimation of monthly rainfall over Japan and surrounding waters from a combination of low-orbit microwave and geosynchronous IR data. J. Appl. Meteor. 32, 335–356. http://dx.doi.org/10.1175/1520-0450(1993)032 < 0335:EOMROJ > 2.0.CO;2.

Ataklti, Y., 2012. Assessing the Potential of GEONETCast Earth Observation and in Situ Data for Drought Early Warning and Monitoring in Tigray and Ethiopia Tewelde. p. 76.

Bargaoui, Z., Chebbi, A., 2009. Comparison of two kriging interpolation methods applied to spatiotemporal rainfall. J. Hydrol., 56–73. http://dx.doi.org/10.1016/j.jhydrol.2008.11.025.

Bargaoui, Z., Tramblay, Y., Lawin, E.A., Servat, E., 2013. Seasonal precipitation variability in regional climate simulations over Northern basins of Tunisia. Int. J. Climatol. 34 (1), 235–248. http://dx.doi.org/10.1002/joc.3683.

Berolo, W., Laborde, J.P., 2003. Statistiques des précipitations journalières extrêmes sur les Alpes-Maritimes, CNRS. P.8.

Bosser P., 2011. Cours d'interpolation spatiale. Ecole Nationale des Sciences Géographiques. p. 53.

Heinemann, T., Lattanzio, A., and Roveda, F., 2002. The EUMETSAT multisensor precipitation estimate (mpe). EUMETSAT Am Kavalleries and 31, 64295 Darmstadt, Germany, p. 8.

Heinemann, T., and Kerényi, J., 2004. The EUMETSAT multisensor precipitation estimate (MPE): concept and validation. EUMETSAT. Am Kavalleries and 31, 64295 Darmstadt, Germany. p. 8.

Hinde, J.P., Demetrio, C.G.B., 1998. Over dispersion: models and estimation. Comput. Stat. Data Anal. 27, 151–170. http://dx.doi.org/10.1016/S0167-9473(98)00007-3.

Ilwis Help, 1999. ILWIS version 2.22 July 1999; On-line Help Web-site: ⟨HTTP://www.itc.nl/ilwis⟩.

La Barbera, P., Lanza, L., and Siccardi, F., 1993. Flash flood forecasting based on multisensor information. Extreme hydrological events: precipitation, floods and droughts. In: Proceedings of the Yokohama Symposium. IAHS Pubf. no. 213, pp. 21–32.

Lafont, D., Guillemet, B., 2004. Beam-filling effect correction with sub-pixel cloud fraction and inhomogeneity parameters using a neural network. J. Geosci. Remote Sens., IEEE Trans. 43 (5), 1070–1077. http://dx.doi.org/10.1109/TGRS.2005.843757.

Orlanski, I., 1975. A rational subdivision of scales for atmospheric processes. Bull. Am. Meteor. Soc. 56, 527–530.

Levizzani, V., Porcù, F., Marzano, F.S., Mugnai, A., Smith, E.A., Prodi, F., 1996. Investigating a SSM/I microwave algorithm to calibrate METEOSAT infrared instantaneous rain rate estimates. Meteorol. Appl. 3, 5–17.

Maathuis, B.P.M., Mannaerts, C.M., Schouwenburg, M., Retsios, B., and Lemmens, R., 2011. GEONETCast Toolbox: Installation, Configuration and User Guide for the GNC Toolbox Plug-in for Ilwis 3.7. Faculty of Geo-information Science & Earth Observation (ITC). University of Twente, Enschede, The Netherlands (Open Source publication available from www.itc.nl).

Nath, S., Mitra, A., Bhowmik, S., 2008. Improving the quality of INSAT derived quantitative precipitation estimates using an neural network method. Geofizika 25 (1), 41–51 , (Retrieved from)http://hrcak.srce.hr/25449.

Oliver, M.A., Webster, R., 1990. Kriging: a method of interpolation for geographical information systems. Int. J. Geogr. Inf. Syst. 4 (3), 313–333. http://dx.doi.org/10.1080/02693799008941549.

Sánchez-Moreno, J.F., Mannaerts, C.M., Jetten, V.G., 2008. Rainfall characterization by satellites and ground data for soil erosion estimation in Cape Verde. In: ACRS 2008: Proceedings of the 29th Asian Conference on Remote Sensing. 10–14 November 2008, Colombo, Sri Lanka. Colombo: Survey Department of Sri Lanka, Asian Association on Remote sensing, 2008. p. 6.

Stein, M.L., 1999. Interpolation of Spatial Data: Some Theory for Kriging. Springer series in statistics, New York, NY, 94.

Todd, M.C., Barrett, E.C., Beaumont, M.J., Bellerby, T.J., 1998. Estimation of daily rainfall over the upper Nile river basin using a continuously calibrated satellite infrared technique. Meteor. Appl. 5, 1–10.

Tsintikidis, D., Haferman, J.L., Anagnostou, E.N., Krajewski, W.F., Smith, T.F., 1997. A neural network approach to estimating rainfall from spaceborne microwave data. J. Geosci. Remote Sens 35 (5), 1079–1093. http://dx.doi.org/10.1109/36.628775.

Thomas, J.G., Craeme, L.S., Thomas, H.V.H., Darren, L.J., 1993. A physical retrieval of cloud liquid water over the global oceans: using special sensor microwave/imager (SSM/I) observations. J. geophys. Res. 98, 471–488.

Turk, F.J., Rohaly, G.D., Hawkins, J., Smith, E.A., Marzano, F.S., Mugnai, A., and Levizzani, V., 1999. Meteorological applications of precipitation estimation from combined SSM/I, TRMM and infrared geostationary satellite data. In: Microwave Radiometry and Remote Sensing of the Earth's Surface and Atmosphere, VSP Int. Sci. Publ., p. 353–363.

Vicente, G.A., 1994. Hourly retrieval of precipitation rate from the combination of passive microwave and infrared satellite measurements (Ph.D. dissertation) 55. Univ. of Wisconsin, Madison, WI, USA, 2796, (Source: Dissertation Abstracts International).